

DEVELOPMENT OF NOVEL ULTRAFINE GRAIN CU METAL MATRIX COMPOSITES REINFORCED WITH Ti-Cu-Co-M (M: Ni, Zr) AMORPHOUS-NANOCRYSTALLINE POWDER

D. Janovszky ^{a*}, F. Kristály ^b, T. Miko ^c, M. Sveda ^a, A. Sycheva ^a

^a MTA-ME Materials Science Research Group, University of Miskolc, Miskolc, Hungary

^b Institute of Mineralogy and Geology, University of Miskolc, Miskolc, Hungary

^c Institute of Physical Metallurgy, Metal Forming and Nanotechnology, University of Miskolc, Miskolc, Hungary

(Received 03 May 2018; accepted 21 September 2018)

Abstract

Novel ultrafine grain composites of Cu matrix reinforced with 2-50 wt. % of $Ti_{48}Cu_{39.5}Ni_{10}Co_{2.5}$ and $Ti_{48}Cu_{39.5}Zr_{10}Co_{2.5}$ (at. %) amorphous-nanocrystalline alloy particles have been fabricated by powder metallurgy. The composites showed a homogeneous structure. The characterization of composites was performed by optical and scanning electron microscopy (SEM), X-ray powder diffraction (XRD), micro- and macrohardness, as well as density measurements. After hot-pressing the crystallite size of Cu was smaller than 200 nm and nanocrystalline phases of reinforcing powder were 5-35 nm. Densities of 97-76 % relative to calculated values of consolidated composites were obtained, depending on the reinforcing weight fraction. Additionally, the mechanical properties and electrical resistivity of composites have been investigated. The results reveal that the 0.2% offset compressive yield strength of composites increases by two and five times, with respect to pure Cu matrix, for the composites reinforced with 2 and 50 wt. % of reinforcing particles, respectively. Electrical resistivity increases continuously, with higher values after 30 wt. % of addition. Changes in mechanical and electrical properties were produced by the increase of amorphous-nanocrystalline additive.

Keywords: Powder metallurgy; Nanostructured materials; Cu-based composite; Mechanical properties; Microstructure; Amorphous materials

1. Introduction

The advantages of copper-based alloys have been long exploited in a wide range of applications, with continuous research on more advanced compositions [1, 2, 3]. Copper itself has attracted much interest due to its excellent thermal and electrical resistivity, ductility and corrosion resistance. In most application fields, both high tensile strengths and high ductility are a constant requirement of the materials. A good solution to overcome this strength-ductility paradox is the fabrication and employment of metal matrix composites (MMCs). The development of Cu-based composites with both high strength and high ductility is a very important research topic. The alloying elements can increase the strength of copper, though by their introduction the electrical resistivity increases significantly. In the case of long-term use of light metal (e.g. Al) based composites strengthening effect of metal can be achieved by uniformly distributed hard materials such as oxides [4, 5, 6], borides [7, 8],

carbides [9, 10] and carbon nanotubes [11]. These additives are also frequently applied in Cu-based composites. Recently, research activity on metallic glass reinforced alloys started; several papers discuss the Al-based metal matrix composites with metallic glass reinforcements, which are promising materials among composites [12, 13, 14]. Metallic glasses have ultra-high hardness, strength (generally more than 1900 MPa), large elastic limit and good corrosion resistance [15, 16]. Unfortunately, bulk metallic glasses (BMGs) still do not display sufficient ductility for industrial applications similar to above mentioned alloys. However, metallic glasses can be used as reinforcements in MMCs, where the high-strength of the glassy phase will be associated with the large deformability of a soft metallic matrix. In addition, the matrix and reinforcement are belonging to the metallic family; an improved interface can be formed between matrix and particles with respect to the more conventional ceramic reinforcements. Cu-based composites with amorphous nanocrystalline

*Corresponding author: fekd@uni-miskolc.hu



reinforcements can be potential application as electrodes for resistance spot and seam welding, different contact materials, various switches, thermal and electric conductors, microwave tubes accelerators, and electrical contacts.

A different research direction of reinforcement for MMCs is the addition of nanocrystalline particles. Such Cu-based metal matrix composites have been extensively studied in recent years due to attained better properties than pure copper [17, 18, 19, 20]. Cu-based composites with nano- Al_2O_3 [21, 22, 23, 24] are materials developed for wide range of applications. Cu-composites with graphene [25, 26, 27] and C-nanotubes [28] have been extensively investigated also. However, producing metallic glasses is an expensive and time-consuming process. Materials similar to metallic glasses are the high amorphous phase containing alloys with moderate to low nanocrystalline phase content, obtained via annealing of amorphous structure or powder metallurgy route. By introducing nanocrystals in situ formed in the glassy matrix, the ductility of BMGs can be improved without sacrificing strength [29, 30]. In nanocrystalline composite alloys, a new strengthening mechanism should be applied due to the smaller size of grain boundaries and grain-boundary segregates. They lead to changes in properties such as grain-boundary energy and cohesive strength, and have an effect on mechanical properties. For instance, grain-size reduction to the nanoscale range (<100 nm) produces very large increases in the strength [31]. Dislocation emission and propagation are essential for nanocrystalline plasticity. Nanocrystalline structure promotes dislocation emission and an increase in the flow stress is required for dislocation propagation [32].

In the case of Cu-based MMCs the possibility of using amorphous-nanocrystalline alloy as reinforcing powders is not reported yet in the literature. Powder metallurgy (P/M) is one of the methods successfully used for the preparation of MMCs in which the materials for reinforcement are uniformly distributed.

In this study, Cu-based MMCs were reinforced with two types of Ti-based amorphous-nanocrystalline particles of composition $\text{Ti}_{48}\text{Cu}_{39.5}\text{Ni}_{10}\text{Co}_{2.5}$ and $\text{Ti}_{48}\text{Cu}_{39.5}\text{Zr}_{10}\text{Co}_{2.5}$ (at. %). The amorphous-nanocrystalline material was obtained by mechanical milling, successfully applied in our laboratory for earlier experiments [33]. The additives were admixed to Cu by ball milling and MMCs have been produced by powder metallurgy. The reason of selecting these alloys as reinforcement is that Ni and Zr have different effect on amorphization of Ti-Cu based alloy during high energy ball milling [33], determined by the heat of mixing (Ni-Ti -35 kJ/mol, Zr-Ti 0 kJ/mol) and atomic properties. The atomic radii are in this case, Ni = 0.124 nm, Cu = 0.128 nm,

Ti = 0.147 nm and Zr = 0.160 nm.

The main objective of this work was to assess the effects of both reinforcing additive fraction ($f = 2, 5, 10, 20, 30, 40$ and 50 wt. %) and the consolidation process (hot-pressing) on the microstructure, mechanical and electrical properties. Electrical resistance of MMCs is expected to increase by the reinforcements [22, 23], a negative effect of additives. To study the variation in electrical resistance the application of at least two additive compositions is required. Because the large difference between Zr (43.3 $\mu\Omega\text{cm}$) and Ni (6.99 $\mu\Omega\text{cm}$), our amorphous-nanocrystalline additives are expected to be suitable materials for the experimental MMCs.

2. Experimental procedures

$\text{Ti}_{48}\text{Cu}_{39.5}\text{Ni}_{10}\text{Co}_{2.5}$ and $\text{Ti}_{48}\text{Cu}_{39.5}\text{Zr}_{10}\text{Co}_{2.5}$ (at. %) amorphous-nanocrystalline alloys were used to prepare reinforcing particles. Cu powder was mixed for 15 min with different amounts of amorphous-nanocrystalline powder ($f = 2, 5, 10, 20, 30, 40$ and 50 wt. %) through high-energy ball milling using a 200-rpm planetary ball mill (Pulverisette 5) under argon atmosphere. The ball-to-powders ratio was 60:1. The oxygen free high conductivity copper powder (OFHC-produced by Alfa Aesar) has spherical structure with an average particle size of 50 μm .

Thermal properties were determined by Netzsch 204 DSC device (40 $^{\circ}\text{C}/\text{min}$, under purified Ar atmosphere). The mixed powders were hot-pressed at 380 $^{\circ}\text{C}$ under 700 MPa pressure for 4 h in high-purity argon atmosphere in order to obtain amorphous/crystalline composites, 3 pieces for each composition. This optimal temperature is high enough to form metallic bonding between the particles and low enough not to allow crystallization of amorphous powders. Cylindrical samples with a diameter and height of 7 mm were produced. After standard metallographic preparation, the microstructure and homogeneity were investigated by optical microscopy (Zeiss Axio Vision V.12).

The microstructure was analyzed by a Hitachi S4800 field emission scanning electron microscope (SEM) equipped with a Bruker AXS Energy-dispersive X-ray spectrometer (EDS) system.

Brinell hardness measurements were performed by a Wolpert UH 930 equipment applying 1 mm diameter ball and a load of 30 kg for 15 s for all composites. The microhardness of initial powders was measured using a load of 50 g for 15 s.

X-ray diffraction (XRD) studies were performed using a Bruker D8 Advance diffractometer (XRD) using Cu K α radiation (40 kV, 40 mA), in parallel beam geometry obtained with Göbel mirror, equipped with a Vantec-1 position sensitive detector (1 $^{\circ}$ window opening), measured in the 2-100 $^{\circ}$ (2 θ)



angular range with a 0.007° (2θ)/29 s speed. The specimen is rotated in sample plane during the measurement, to obtain data from the whole surface and to reduce in plane preferred orientation effects. Rietveld refinement was done in TOPAS4 software with empirical instrumental profile obtained on SRM640a Si standard.

The relative density of the composites was measured according to Archimedes' principle. The electrical resistivity of copper alloy (OFHC), hot pressed copper and composites of various reinforcement content was determined by using a Thomson bridge and a Keithley 2182A type of nanovoltmeter.

Compression tests were carried out by an Instron 5982 electromechanical universal material testing equipment with a strain rate of $1 \times 10^{-2} \text{ s}^{-1}$ at room temperature. The maximal logarithmic strain was 0.5. To decrease friction, we used consistent grease. Three samples of each composition were measured.

3. Results and Discussion

3.1 Powder characterization

Representative SEM images illustrating the morphology of the initial Cu and two amorphous-nanocrystalline powders are shown in Fig. 1. The as-received Cu powder consists of spherical particles (see Fig. 1a), with an average size of $50 \mu\text{m}$ (as stated by the producer). Median particle size (by laser scattering size analysis) of $\text{Ti}_{48}\text{Cu}_{39.5}\text{Ni}_{10}\text{Co}_{2.5}$ and $\text{Ti}_{48}\text{Cu}_{39.5}\text{Zr}_{10}\text{Co}_{2.5}$ is 58.4 and $84.6 \mu\text{m}$, from our previous investigations [33]. The grains of amorphous-nanocrystalline powders, produced by applying 15 h of high-energy ball-milling, have irregular shape. The onset of crystallization is 394°C and 387°C for $\text{Ti}_{48}\text{Cu}_{39.5}\text{Ni}_{10}\text{Co}_{2.5}$ and $\text{Ti}_{48}\text{Cu}_{39.5}\text{Zr}_{10}\text{Co}_{2.5}$, respectively based on DSC measurement [33].

As determined from XRD data by Rietveld refinement (Fig. 2a) the structure of $\text{Ti}_{48}\text{Cu}_{39.5}\text{Ni}_{10}\text{Co}_{2.5}$ powder is not fully amorphous, with 87 wt. % amorphous, and two nanocrystalline phases, $\text{CuTi}_3(\text{Ni})$ and Ti_2CuNi remained in the powder. From peak broadening data the crystallite size is $17.00-$

30.00 nm and $15.00-20.00 \text{ nm}$, respectively. In the case of $\text{Ti}_{48}\text{Cu}_{39.5}\text{Zr}_{10}\text{Co}_{2.5}$ powder 40 wt. % is amorphous and also two nanocrystalline phases were formed. H2 ($\text{P63}/\text{mmc}$) and Cu_7ZrTi_3 ($\text{P4}/\text{mmm}$) phases can be detected by XRD (Fig. 2b). H2 hexagonal phase was identified based on data reported in [34].

3.2 Microstructure of hot-pressed composites

Particle clustering is a major problem in production of homogeneous particle distribution of reinforced composites. The typical microstructure of the hot-pressed composites with $f = 20$ and 40 wt. % amorphous-nanocrystalline fracture is illustrated in Fig. 3. It can be observed that the reinforcing particles are arranged almost randomly in all samples. Particle clustering is observed particularly in the case of higher mass fraction of amorphous-nanocrystalline reinforcement addition. The clustering already occurs in the dry powder and milling also, creating difficulties in composite homogenization (Fig. 3a, b insets). The cold-welding mechanism during milling has a particularly dominant effect on the particles of $\text{Ti}_{48}\text{Cu}_{39.5}\text{Zr}_{10}\text{Co}_{2.5}$ and causes formation of closed pores between and in the particles. The average distance between reinforcing particles in the $f = 40$ wt. % composite is $45 \mu\text{m}$ and $40 \mu\text{m}$ for $\text{Ti}_{48}\text{Cu}_{39.5}\text{Ni}_{10}\text{Co}_{2.5}$ and $\text{Ti}_{48}\text{Cu}_{39.5}\text{Zr}_{10}\text{Co}_{2.5}$ powders, respectively. Namely, the average distance between reinforcing particles is of the same size as initial Cu average particle size in the powder.

Both types of amorphous-nanocrystalline particles partially crystallize during the hot-pressing based on the XRD analysis (Fig. 4) owing to hot-pressing. In composites with $\text{Ti}_{48}\text{Cu}_{39.5}\text{Ni}_{10}\text{Co}_{2.5}$ reinforcement the initial $\text{CuTi}_3(\text{Ni})$ phase decomposes into $\gamma\text{-CuTi}$ ($\text{P4}/\text{nm}$) and $\delta\text{-CuTi}$ ($\text{P4}/\text{mmm}$) phases. The Ti_2CuNi phase in particles is unchanged. Based on XRD analysis the Cu matrix dissolves some Ni or Co (separately or together), indicated by the appearance of an alloyed Cu structure (Cu-alloyed in Table 1). The peaks of Cu have shifted to lower angles, the lattice parameter of Cu-matrix and Cu-alloyed are 0.3616 nm and 0.3613 nm , respectively. These

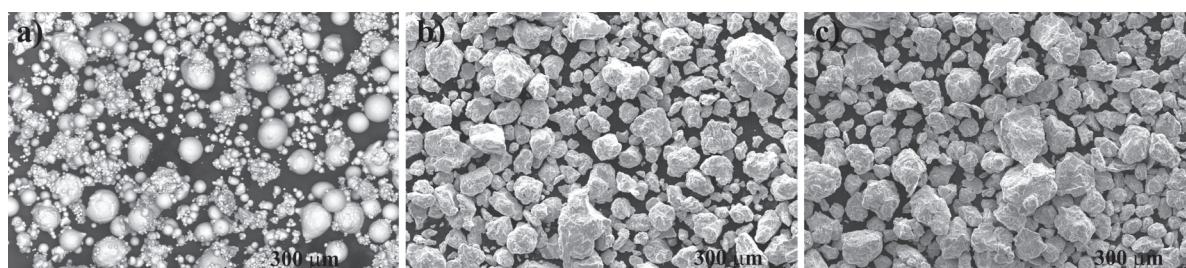


Figure 1. SEM (secondary electron) micrographs showing the (a) morphology of as-received gas-atomized Cu powder (b) $\text{Ti}_{48}\text{Cu}_{39.5}\text{Ni}_{10}\text{Co}_{2.5}$ and (c) $\text{Ti}_{48}\text{Cu}_{39.5}\text{Zr}_{10}\text{Co}_{2.5}$ powders



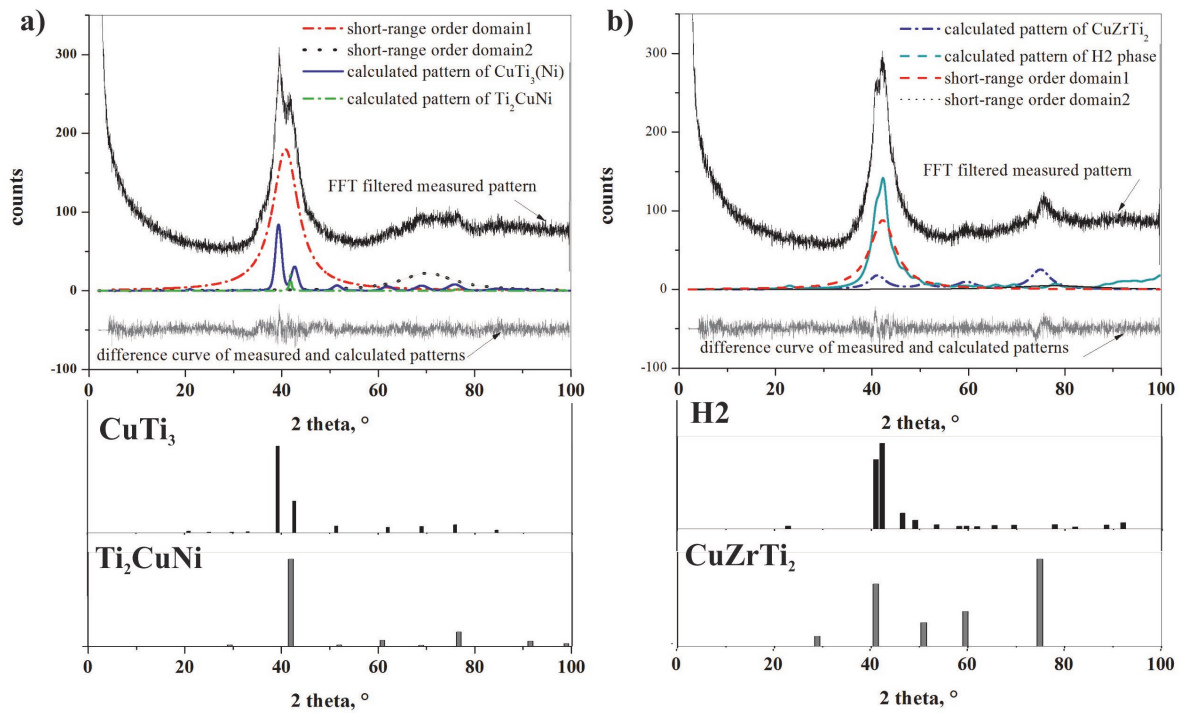


Figure 2. Calculated phase peaks and amorphous halo of (a) $Ti_{48}Cu_{39.5}Ni_{10}Co_{2.5}$ and (b) $Ti_{48}Cu_{39.5}Zr_{10}Co_{2.5}$ powders

observations suggest that a diffusion process takes place between the Cu matrix and reinforcing particles, confirmed by the crystallization of new phases. In the case of 40 wt. % $Ti_{48}Cu_{39.5}Ni_{10}Co_{2.5}$ reinforcement the weight ratio and the crystallite sizes of phases are summarized in Table 1. The Cu-matrix remained

ultrafine grained structure. The composition and structure of amorphous phase is modified under hot-pressing, deduced from the changes of amorphous halos maximum positions [34, 35]. The first peak position of amorphous halo is 0.2212 nm before hot-pressing and 0.2128 nm after hot-pressing, indicating

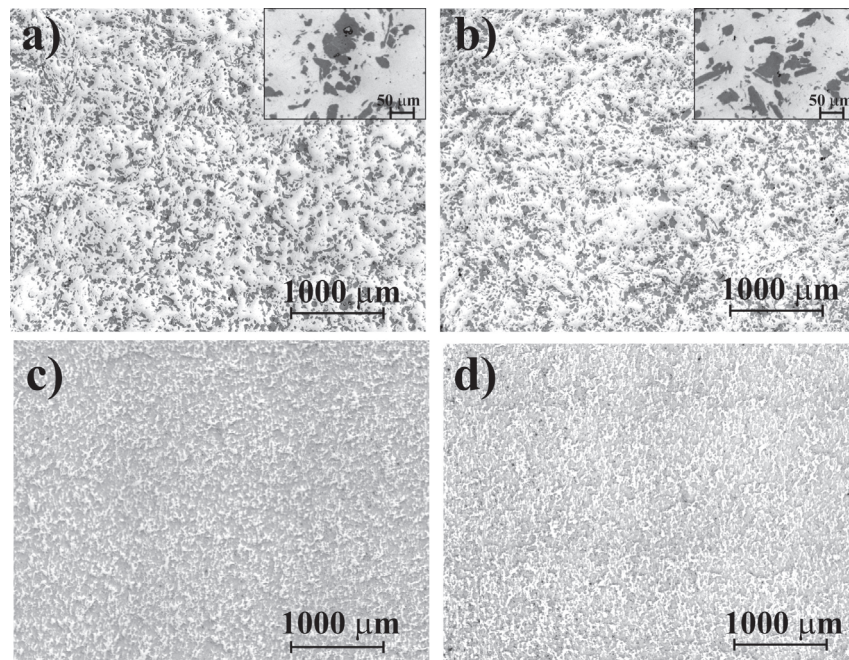


Figure 3. Optical micrographs of cross sections for the consolidated composites reinforced with $f=20$ (a, b) and $f=40$ wt. % (c, d) of $Ti_{48}Cu_{39.5}Ni_{10}Co_{2.5}$ (a, c) and $Ti_{48}Cu_{39.5}Zr_{10}Co_{2.5}$ glassy powders (b, d)

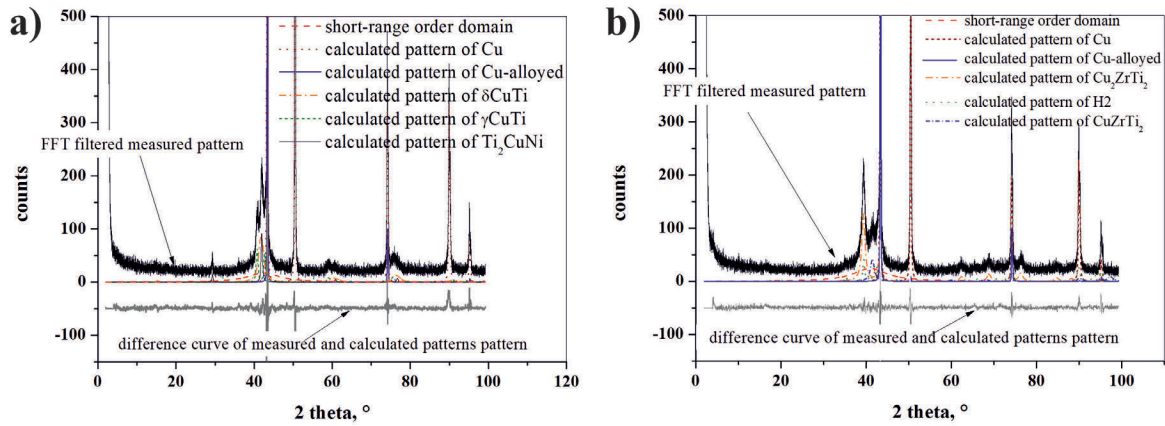


Figure 4. XRD patterns of initial amorphous-nanocrystalline powders and composites (a) with $Ti_{48}Cu_{39.5}Ni_{10}Co_{2.5}$ and (b) $Ti_{48}Cu_{39.5}Zr_{10}Co_{2.5}$ reinforcements

the removal of the larger atom (Ti) from the amorphous structure. These modifications are owing to deformation and heating process, explaining the Ti source for the newly crystallized CuTi products.

In the case of $Ti_{48}Cu_{39.5}Zr_{10}Co_{2.5}$ reinforcement the

Table 1. Parameters of the phases based on the XRD analysis in the case of 40 wt. % $Ti_{48}Cu_{39.5}Ni_{10}Co_{2.5}$ composite

phases	fraction, wt. %		crystallite size, nm	
	before hot-pressing	after hot-pressing	before hot-pressing	after hot-pressing
amorphous structure	34.8	12	-	-
Cu-matrix	60	59	626-983	125-196
Cu-alloyed	0	1	0	630-1 000
δ -CuTi	0	18.1	0	5-8
γ -CuTi	0	8.1	0	22-35
Ti_2CuNi	1.2	1.8	15-20	21-33
$CuTi_3$	4	0	17-30	-

Table 2. Parameters of the phases based on the XRD analysis in the case of 40 wt. % $Ti_{48}Cu_{39.5}Zr_{10}Co_{2.5}$ composite

phases	fraction, wt. %		crystallite size, nm	
	before hot-pressing	after hot-pressing	before hot-pressing	after hot-pressing
amorphous structure	18	18	-	-
Cu-matrix	60	50.2	626-983	68-107
Cu-alloyed	0	8	0	630-1 000
Cu_2ZrTi_2	0	21.4	0	6-11
H2 ($Ti_{34.90 \pm 1.1}Cu_{46.1 \pm 1.0}Zr_{17.4 \pm 0.4}Co_{1.6 \pm 0.2}$)	14	1.2	0	13-20
Ti_2CuZr	8	1.2	15-20	5-8

diffusion process between the Cu matrix and the reinforcing particles is more pronounced, leading to significant crystallization of newly formed phases (Table 2). Cu_2ZrTi_2 phase crystallizes in the course of hot-pressing on the expense of H2 and Ti_2CuZr phases, their amount decreases compared to the initial amorphous-nanocrystalline material. The composition and structure of amorphous phase is also changed, but differently from the Ni-containing composite. The peak position of amorphous halo is to 0.2142 nm before hot-pressing, modified to 0.2204 nm after hot-pressing, explained by the removal of Cu atoms.

3.3 Physical properties of composites

The effect of amorphous-crystalline particle content on density of the composites is plotted in Fig. 5a. The density continuously decreases with increasing reinforcement content owing to the lower density of amorphous alloys than copper. The theoretical density of the composite test pieces was calculated from the simple rule of mixtures taking into account the theoretical values for copper (8.96 g/cm³) and master alloy of amorphous-nanocrystalline powder (6.35 and 6.22 g/cm³ for $Ti_{48}Cu_{39.5}Ni_{10}Co_{2.5}$ and $Ti_{48}Cu_{39.5}Zr_{10}Co_{2.5}$, respectively). The density of hot-pressed pure Cu-sample is 8.81 g/cm³, which is 2% less than the density of bulk Cu, due to porosity maintained between grains. As a general observation, it can be said that the deviation from the theoretical density is higher in the case of composites containing $Ti_{48}Cu_{39.5}Zr_{10}Co_{2.5}$, confirming the statement about closed pores based on the microstructure. The $\Delta\rho/\rho_{th}$ of metal matrix composites can be calculated from Eq. (1):

$$\Delta\rho / \rho_{th} = [100 * (\rho_{th} - \rho_{h-pressed}) / \rho_{th}] \quad (1)$$

where ρ_{th} is the theoretical density, $\rho_{h-pressed}$ is the density of hot-pressed sample.



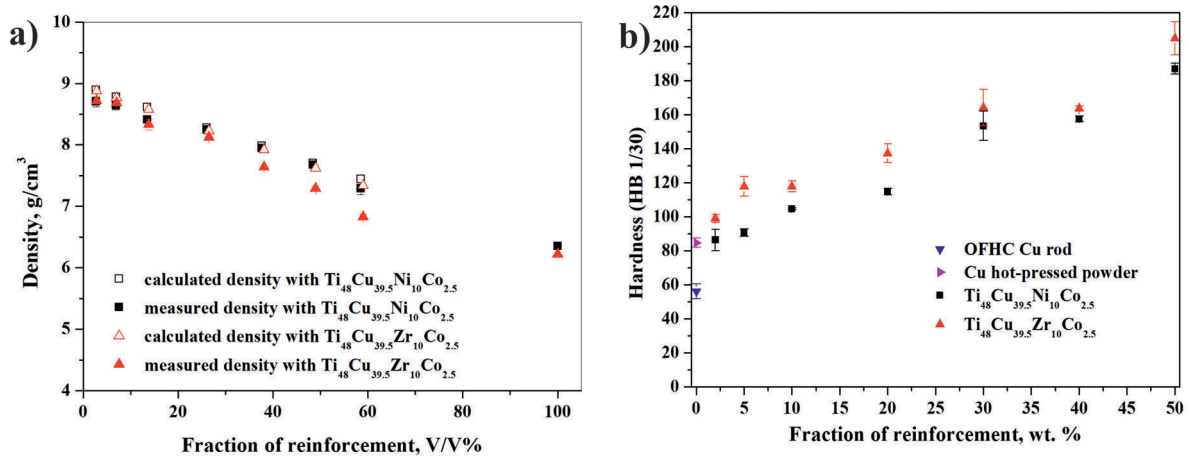


Figure 5. Effect of reinforcement content on (a) the density and (b) Brinell hardness of the hot-pressed Cu-based composites

In the case of composites with Ti₄₈Cu_{39.5}Ni₁₀Co_{2.5} reinforcement, the values of $\Delta\rho/\rho_{th}$ are below 5 % (Table 3). However, these values of Cu-Ti₄₈Cu_{39.5}Zr₁₀Co_{2.5} composites vary from 1.58 to 9.96 %. In both cases, the $\Delta\rho/\rho_{th}$ increases with increasing the reinforcement content, explained mainly by the increase in intergranular porosity.

Hardness examinations have shown significant

reinforcement effects, composite materials have higher hardness compared to pure hot-pressed Cu-powder and oxygen free copper (OFHC) rod (Fig. 5b). The increase in the composite hardness is caused by the fact that the hardness of amorphous-nanocrystalline phases is much higher than that of copper. Comparing the effect of reinforcing phases, it can be established that the values of hardness show

Table 3. Physical properties of hot-pressed samples

Reinforcing content (wt %)	Composition of reinforcing powder (at. %)	Archimedes' Density (g/cm ³)	Relative density (%)	$\Delta\rho/\rho_{th}$ (%)	Specific electrical resistivity ($\mu\Omega\cdot\text{cm}$)	%IACS
0	OFHC rod	8.96 ± 0.06	100.00 ± 0.62	0	1.72 ± 0.04	98.76 ± 2.44
	Hot-pressed powder	8.81 ± 0.11	98.33 ± 1.23	1.66	2.38 ± 10.14	70.86 ± 5.17
2	Ti ₄₈ Cu _{39.5} Ni ₁₀ Co _{2.5}	8.70 ± 0.08	97.10 ± 0.89	2.32	3.17 ± 0.16	53.03 ± 2.75
	Ti ₄₈ Cu _{39.5} Zr ₁₀ Co _{2.5}	8.72 ± 0.01	97.32 ± 0.11	2.08	3.07 ± 0.18	55.00 ± 3.13
5	Ti ₄₈ Cu _{39.5} Ni ₁₀ Co _{2.5}	8.64 ± 0.07	96.43 ± 0.78	2.16	3.75 ± 0.43	45.31 ± 5.58
	Ti ₄₈ Cu _{39.5} Zr ₁₀ Co _{2.5}	8.68 ± 0.09	96.88 ± 1.00	1.58	4.24 ± 0.26	38.98 ± 1.92
10	Ti ₄₈ Cu _{39.5} Ni ₁₀ Co _{2.5}	8.41 ± 0.02	93.86 ± 0.22	3.31	4.03 ± 0.08	41.61 ± 0.84
	Ti ₄₈ Cu _{39.5} Zr ₁₀ Co _{2.5}	8.33 ± 0.09	92.97 ± 1.00	4.12	5.73 ± 0.46	29.44 ± 2.43
20	Ti ₄₈ Cu _{39.5} Ni ₁₀ Co _{2.5}	8.13 ± 0.16	90.74 ± 1.79	3.64	5.07 ± 0.20	33.16 ± 1.73
	Ti ₄₈ Cu _{39.5} Zr ₁₀ Co _{2.5}	8.12 ± 0.02	90.63 ± 0.22	3.41	6.75 ± 0.61	24.98 ± 2.26
30	Ti ₄₈ Cu _{39.5} Ni ₁₀ Co _{2.5}	7.95 ± 0.02	88.73 ± 0.22	2.8	7.79 ± 0.34	21.61 ± 0.97
	Ti ₄₈ Cu _{39.5} Zr ₁₀ Co _{2.5}	7.64 ± 0.01	85.27 ± 0.11	6.15	10.43 ± 1.16	16.23 ± 1.75
40	Ti ₄₈ Cu _{39.5} Ni ₁₀ Co _{2.5}	7.68 ± 0.01	85.71 ± 0.11	3.04	13.27 ± 1.47	12.80 ± 1.46
	Ti ₄₈ Cu _{39.5} Zr ₁₀ Co _{2.5}	7.29 ± 0.03	81.36 ± 0.33	7.3	17.34 ± 1.37	9.72 ± 0.74
50	Ti ₄₈ Cu _{39.5} Ni ₁₀ Co _{2.5}	7.29 ± 0.10	81.36 ± 1.12	4.76	17.50 ± 0.92	9.63 ± 0.48
	Ti ₄₈ Cu _{39.5} Zr ₁₀ Co _{2.5}	6.83 ± 0.04	76.28 ± 0.47	9.96	27.79 ± 3.30	6.10 ± 0.70

Table 4. The electrical conductivity (λ) and mechanical properties of the Cu-based composites

Reinforcing phase in Cu matrix	fraction of reinforcement	λ , % IACS	Hardness	Yield strength, MPa	Rp0.2, Mpa	Reference
ultrafine Al ₂ O ₃ particles	1 vol. %	51-52	115 HB	288		[36]
Al ₂ O ₃ nanoparticles	2.75 vol. %	85	86 HB	533		[23]
Al ₂ O ₃ nanoparticles	1 vol. %	62			394	[22]
	2 vol. %	59			501	
	5 vol. %	56			580	
Al ₂ O ₃ nanoparticles	1.0 wt. %	54-60	40-54 HRF (43-54 HB)			[37]
			38-48 HRF (42-50 HB)			
	2.0 wt. %	29-41	13-42 HRF (max 44 HB)			
Al ₂ O ₃ nanoparticles	1 vol. %	50.7 (34 nΩm)			460	[39]
	5 vol. %	44.2 (39 nΩm)			620	
nanographite	0.5-5.0 wt. %	76.9-68.3	27-20 HB			[28]
graphene nanosheets	0.5-5.0 wt. %	78.5-61.5	33-27 HB			
carbon nanotubes	0.5-5.0 wt. %	74.6-5.3	30-15 HB			
TiO ₂ nanoparticles	2.5 wt. %	78	115 HB	299		[40]
	5 wt. %	69.5	167 HB	327		
	7.5 wt. %	49	209 HB	370		
Ti ₄₈ Cu _{39.5} Ni ₁₀ Co _{2.5}	2 wt. %	53	86 HB		210	present study
	5 wt. %	45	90 HB		249	
	10 wt. %	41	105 HB		253	
Ti ₄₈ Cu _{39.5} Zr ₁₀ Co _{2.5}	2 wt. %	55	99 HB		253	
	5 wt. %	39	118 HB		332	
	10 wt. %	29	118 HB		270	

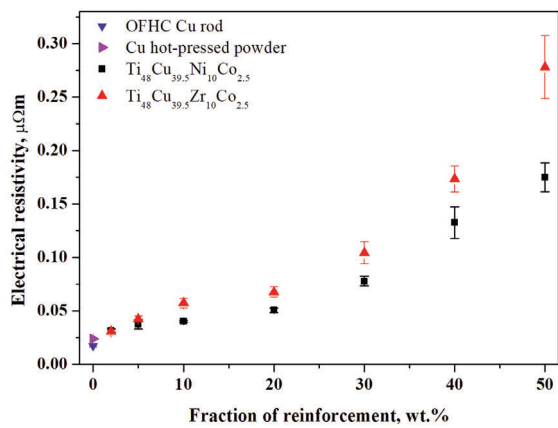


Figure 6. Dependency of electrical resistivity of composites on the reinforcement content

great diversity in the case of nano-Al₂O₃ containing composites (Table 4). The hardness depends on the method of production and nature of initial phases, in contrast with electrical resistivity, which is increasing regardless the technology and additives. Using carbon nanotubes, nanographite or graphene nanosheets the electrical resistivity does not deteriorate significantly. However, at the same time, hardness does not improve (Table 4). The Cu-2.5 wt. % TiO₂ nanocomposite prepared by thermochemical process has good mechanical properties and reasonable electrical resistivity, but the production process is complicated [37]. In the present study, the hardness of the composites containing amorphous-nanocrystalline phases is increased from 86 HB to 210 HB with increasing additive ratio.

Resistivity is affected by the chemical composition and microstructure of compact materials.



It is well known that the resistivity and hardness exhibit a parallel trend. Generally, the electrical resistivity of amorphous-nanocrystalline particles is higher than that of pure Cu. The total resistivity of Cu-based reinforced composite is influenced by the resistivity of Cu matrix, determined by dislocations, grain boundaries, interfaces, impurities and reinforcing materials [17]. It is observed that the increase of reinforcement content in the Cu matrix leads to an increase of electrical resistivity values. In our experiments, the electrical resistivity changes exponentially with the reinforcement content of the Cu-based composites (Fig. 6). The values of resistivity obtained in the $\mu\Omega\text{cm}$ units were converted to % IACS conductivity values. The electrical conductivity changes from 53 to 9% IACS and from 55 to 6% IACS for $\text{Ti}_{48}\text{Cu}_{39.5}\text{Ni}_{10}\text{Co}_{2.5}$ and $\text{Ti}_{48}\text{Cu}_{39.5}\text{Zr}_{10}\text{Co}_{2.5}$ samples, respectively (Table 4). This change is not only due to the higher resistivity of reinforcing particles compared with pure Cu, but also to the increase of resistivity Cu with higher additive amounts, alloying and development of lattice defects. In accordance, the electrical conductivity of pure hot-pressed Cu is 71% IACS. The value of resistivity can be decreased by increasing the pressing temperature. The onset of crystallization temperature for both composites is $\sim 390^\circ\text{C}$ (determined by DSC), so the hot-pressing temperature cannot be increased. Considering the effect of two different reinforcing compositions, it can be observed that the Zr ($\rho = 43.3 \mu\Omega\text{cm}$) containing particles stronger enhance the electrical resistivity than the Ni ($\rho = 6.99 \mu\Omega\text{cm}$) containing particles in the case of $f = 10$ wt. %. However, by increasing the ratio of the reinforcement particles, this difference is constantly diminished. This process is only possible if a significant portion of porosity in $\text{Cu-Ti}_{48}\text{Cu}_{39.5}\text{Zr}_{10}\text{Co}_{2.5}$ composites is located between and within amorphous particles, thus contributing less to the decrease in resistivity.

Furthermore, in the case of Zr bearing additive the Cu-alloyed fraction is higher than for Ni bearing additive. Since electrical resistivity is lower for Ni-composites, our data confirm that the dissolved elements in Cu matrix significantly increase the

resistivity [38].

For all examined composites, the amount of Fe impurity is approximately equal, linearly increasing the electrical resistivity with increasing concentration in the Cu-based solid solution [36]. Fe content is 0.2-0.8 wt. % based on EDX measurements, and this impurity also induces a few percent IACS increase in electrical conductivity which is inversion of resistance.

3.4 Mechanical properties and fracture surfaces of the hot-pressed composites

In order to compare the data of composites with those of pure Cu-phase, the true stress versus logarithmic strain response in uniaxial compression under quasistatic loading are plotted together with the curves for the hot-pressed Cu-powder and OFHC rod (Fig. 7). The mechanical properties of pure ultrafine grained Cu are improved by the addition of both types of amorphous-nanocrystalline reinforcement. The 0.2% offset in compressive yield strength $R_{p0.2}$ (MPa) of hot-pressed Cu-powder sample is 115 MPa which is ~ 20 MPa than softened OFHC copper rod. Both amorphous-nanocrystalline additives greatly increase this value, in the case of $f = 50$ wt. % $\text{Ti}_{48}\text{Cu}_{39.5}\text{Ni}_{10}\text{Co}_{2.5}$ and $\text{Ti}_{48}\text{Cu}_{39.5}\text{Zr}_{10}\text{Co}_{2.5}$ content the $R_{p0.2}$ is 526 MPa and 643 MPa, respectively (Table 5). Both types of compositions up to $f = 20$ wt. % show a work hardening-like behavior for large strains. In the case of composites with $\text{Ti}_{48}\text{Cu}_{39.5}\text{Ni}_{10}\text{Co}_{2.5}$ reinforcing contents with $f = 2, 5, 10$ and 20 wt. % the compression tests have been interrupted at 0.5 logarithmic strain because they behaved like pure copper samples. However, the absolute values of their strength were higher than those of pure Cu-matrix (as work-hardening materials) (Fig. 7a). These composite materials display fairly large plastic deformation. The true stress versus logarithmic strain of composites with $f = 30, 40$ and 50 wt. % $\text{Ti}_{48}\text{Cu}_{39.5}\text{Ni}_{10}\text{Co}_{2.5}$ reinforcement contents display local maximum, which corresponds to maximum compressive strength value. The compressive strength rises to 652 MPa in the case of $f = 50$ wt. %, the highest for all Ni-

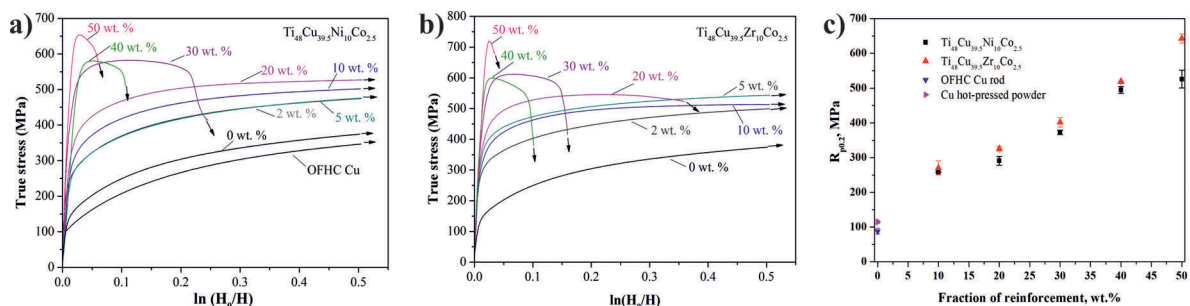


Figure 7. Compressive stress-strain curves of the composites: (a) reinforcing particle $\text{Ti}_{48}\text{Cu}_{39.5}\text{Ni}_{10}\text{Co}_{2.5}$; (b) $\text{Ti}_{48}\text{Cu}_{39.5}\text{Zr}_{10}\text{Co}_{2.5}$; (c) 0.2% offset of compressive yield strength

Table 5. Data on compressive strength and plastic strain of the composites depending on fraction of the reinforcement

	Reinforcing content (wt. %)	2	5	10	20	30	40	50
$R_{p0.2}$, MPa	$Ti_{48}Cu_{39.5}Ni_{10}Co_{2.5}$	210 ± 0.3	249 ± 21.2	253 ± 0.1	291 ± 12.6	373 ± 6.3	495 ± 9.8	526 ± 25.6
	$Ti_{48}Cu_{39.5}Zr_{10}Co_{2.5}$	253 ± 0.6	332 ± 24.8	270 ± 20.4	325 ± 6.3	401 ± 13.2	519 ± 1.0	643 ± 13.3
Compressive strength (MPa)	$Ti_{48}Cu_{39.5}Ni_{10}Co_{2.5}$	>	>	>506	>512	579 ± 4	579 ± 2	652 ± 2
	$Ti_{48}Cu_{39.5}Zr_{10}Co_{2.5}$	>	>	>511	551 ± 8	615 ± 3	597 ± 1	717 ± 4
Plastic strain, %	$Ti_{48}Cu_{39.5}Ni_{10}Co_{2.5}$	>40	>40	>40	>40	11.7 ± 0.9	5.6 ± 0.1	4.8 ± 0.3
	$Ti_{48}Cu_{39.5}Zr_{10}Co_{2.5}$	>40	>40	>40	20.5 ± 1.8	6.5 ± 0.1	4.2 ± 1.0	3.2 ± 0.2

containing compositions.

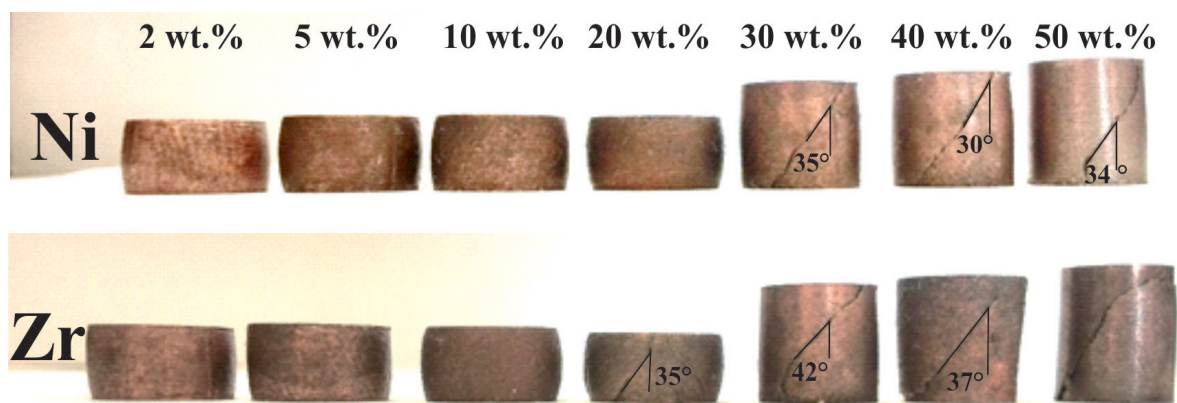
However, for the composite reinforced with $f = 30, 40$ and 50 wt. % of amorphous-nanocrystalline powder, the stress, after reaching the maximum value gradually decreases with increasing strain through the propagation of cracks.

The 0.2% offset compressive yield strength $R_{p0.2}$ (MPa) of the composite with $f = 2, 5$ and 10 wt. % $Ti_{48}Cu_{39.5}Zr_{10}Co_{2.5}$ is 253 MPa, 332 MPa and 270 MPa, respectively. These compositions show a work hardening-like behavior for large strains and the compression tests have been interrupted at 0.5 logarithmic strain. The 0.2% offset compressive yield strength increases almost linearly from 253 MPa for the sample with $f = 2$ wt. % of reinforcing particles to 643 MPa for the composite with $f = 50$ wt. % reinforcement (Fig. 7c). The compression curves of more than $f = 10$ wt. % of $Ti_{48}Cu_{39.5}Zr_{10}Co_{2.5}$ content have a local maximum (Fig. 7b), which means that deformation ability of the composite is exhausted, resulting in crack development. The compressive strength with $f = 20$ and 50 wt. % is 551 and 717 MPa, respectively (Table 5).

An obvious trend has been observed with respect to the reinforcing particle content and mechanical properties in series of Cu composites. The compressive stress-strain curves revealed promising strength enhancements by increasing the fraction of

both reinforcing particles and parallel to this the ductility decreases applying $f = 30$ wt. % and more of amorphous-nanocrystalline particles. Both type of reinforcing particles is promising for improving the mechanical properties of the ultrafine grained Cu-matrix, which indicates that the reinforcing particles are an effective strengthening agent for Cu matrix (Fig. 4c). In the case of Ni content cracks appear only in the sample with $f = 30$ wt. % of reinforcing particles. In contrast, when the Ni content is replaced with Zr in the reinforcing material, the cracks are clearly visible on the surface of compressed composites with 20 wt. % additive (Fig. 8). It can be observed that the fracture plane of rod sample is close to 45° relative to the load direction.

The deformation of composites is very complicated and depends on the size and type of reinforcing particles. The strengthening effect of particles in a metal matrix composite can be attributed to direct and indirect strengthening effects [41]. The applied load is transferred from the matrix to the hard particles - this is the direct strengthening effect. The deformation of the soft matrix is significantly affected by the presence of hard reinforcements, the particles obstruct the dislocation movement - this is the indirect strengthening effect. The stress arises at the interface between the matrix and particles, and its distribution is inhomogeneous in the composite with

**Figure 8.** Macrographs of the compressed samples containing $Ti_{48}Cu_{39.5}Ni_{10}Co_{2.5}$ and $Ti_{48}Cu_{39.5}Zr_{10}Co_{2.5}$ particles

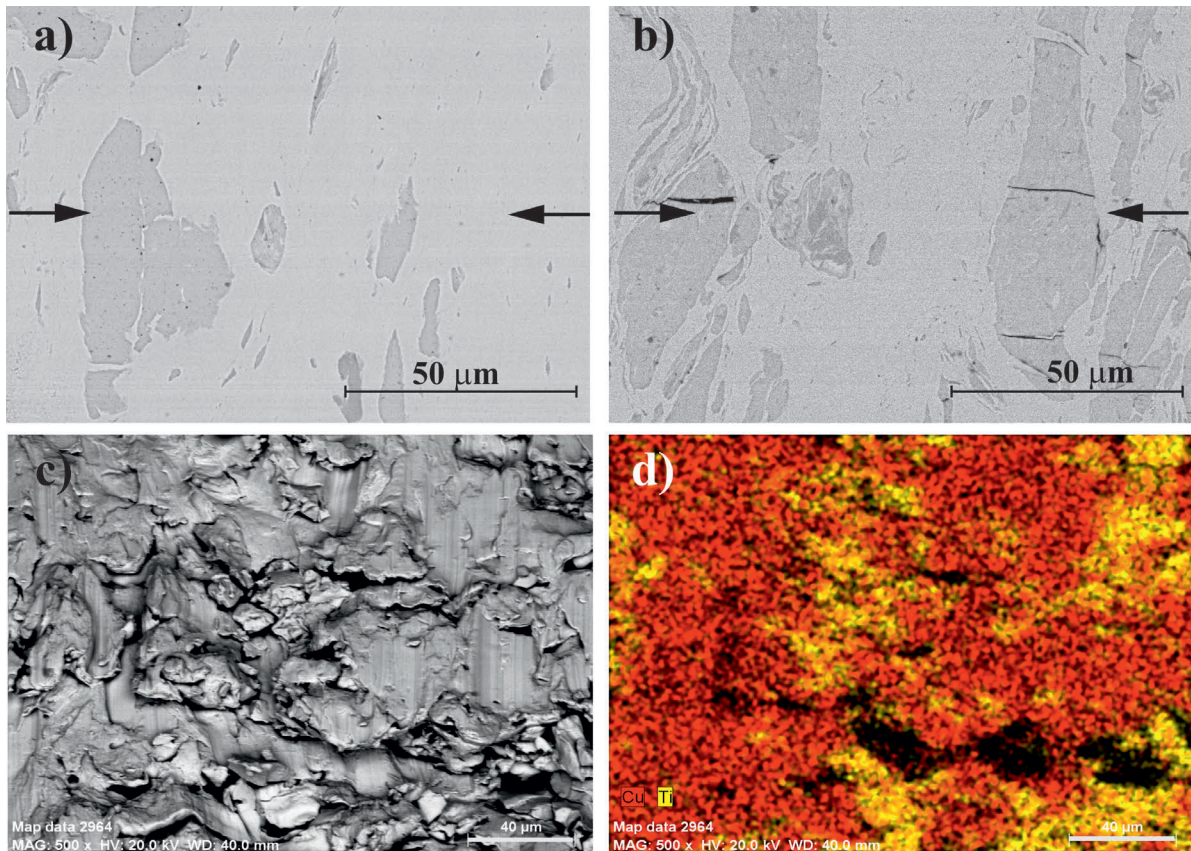


Figure 9. Fracture surface after compression tests of the composites reinforced with (a) 5 and (b, c, d) 30 wt. % of $Ti_{48}Cu_{39.5}Zr_{10}Co_{2.5}$ particles; (a, b) microstructure of polished surface, (c, d) fracture surface and EDS elemental map of the same area; compression direction is indicated by arrows

hard particles.

In the case of low reinforcement content (2, 5 and 10 wt. %), the compressive load cannot be effectively transferred from the Cu-matrix to the hard particles. But the amorphous-crystalline particles have been plastically deformed and a few particles have broken (Fig. 9a). No indication of particle–matrix debonding is observed. At high reinforcement content, the load is shared by the matrix and the amorphous-nanocrystalline particles, leading to significant particle deformation as it can be seen on polished surface of composite with $f = 30$ wt. % $Ti_{48}Cu_{39.5}Zr_{10}Co_{2.5}$ particle (Fig. 9b). The image reveals that, after deformation, several cracks appear in the reinforcing particles (Fig. 9b). Cracks in the particles of both type of composites occur parallel to the compression direction (indicated by arrows in Fig. 9a, b) which is defined as distensile fracture [42]. In contrast, the cracks are not observed at the particle–matrix interface, good interfacial bonding appears between the matrix and reinforcement. The soft Cu penetrates the broken reinforcement particles and the matrix undergoes large plastic deformation (Fig. 9c). At higher volume fractions, the particles may form a continuous network. The fraction of both

reinforcement particles required to extremely decrease the ductility of composites (percolation limit) is about 40 wt. % based on the compression test (Fig. 7). In both reinforcing materials, the distance between reinforcing particles is of the same size as initial Cu powder grain size. Composites with 50 wt. % reinforcement hardly show a plastic deformation. Deformation twinning, as a frequent deformation mechanism in copper metal, was not observed because of the ultrafine nature of copper grains.

4. Conclusions

Novel Cu-matrix composites reinforced by 2-50 wt. % of amorphous-nanocrystalline particles $Ti_{48}Cu_{39.5}Ni_{10}Co_{2.5}$ and $Ti_{48}Cu_{39.5}Zr_{10}Co_{2.5}$ (at. %) have been synthesized by powder metallurgy, through hot-pressing, preserving the ultrafine grain size of Cu matrix. The amorphous-nanocrystalline particles were partly devitrified with nanometric crystallite sizes at the level of 5-35 nm. The reinforcing particles were distributed homogeneously in the matrix after hot-pressing. The relative density of composites varied from 97 to 76 % (relative to Cu) depending on the weight fraction and type of addition. Results showed

that with increasing the content of reinforcing particles, the composites exhibited extremely high strength and hardness. The hardness of the composites is always higher than 90 HB if the reinforcement content is above $f = 5$ wt. %. In the case of $f = 50$ wt. % $\text{Ti}_{48}\text{Cu}_{39.5}\text{Ni}_{10}\text{Co}_{2.5}$ containing composite the maximum compressive strength was 653 MPa. The composite with $f = 50$ wt. % $\text{Ti}_{48}\text{Cu}_{39.5}\text{Zr}_{10}\text{Co}_{2.5}$ demonstrated 715 MPa the maximum compressive strength. The electrical resistivity of the composites strongly depends on the type and fraction of amorphous-crystalline particles. Ni as alloying element is more suitable than Zr considering the electrical resistivity in potential application as contact materials. The optimal concentration of reinforcing particles is about 5 wt. %; further increase of their concentration leads to significant increase of resistivity. Considering all the composites obtained in the current research, 5 wt. % amorphous-nanocrystalline composite reinforced by $\text{Ti}_{48}\text{Cu}_{39.5}\text{Ni}_{10}\text{Co}_{2.5}$ has more than double hardness and 0.2% offset compressive yield strength $R_{p0.2}$ (MPa) compared to pure copper. However, the resistivity of this composite is $3.75 \mu\Omega\text{cm}$, which is naturally higher than pure copper.

Good interfacial bonding was observed between the matrix and both reinforcements.

All the results showed that amorphous-nanocrystalline particles are promising alternative reinforcement materials for Cu-based composites, with significantly improved mechanical properties, which may lead to the development of modern types of composites. As a result, varying the nature and the weight fraction of reinforcing particles one can achieve a good balance between strength and electrical resistivity depending on application field of composites.

Acknowledgement

This article was carried out as part of the GINOP-2.3.2-15-2016-00027 project implemented in the framework of the Szechenyi 2020 program. The realization of this project is supported by the European Union.

References

- [1] X. Qu, L. Zhang, M. Wu, S. Ren, Prog. Nat. Sci. Mater. Int., 21 (2011) 189-197.
- [2] R. Li, H. Kang, Z. Chen, G. Fan, C. Zou, W. Wang, S. Zhang, Y. Lu, J. Jie, Z. Cao, T. Wang, Sci. Rep., 6, 20799; doi: 10.1038/srep20799 (2016).
- [3] D. Zhou, W. Zeng, D. Zhang, J. Alloys. Compd., 682 (2016) 590-593.
- [4] Q. Han, R. Setchi, S. L. Evans, Powder. Technol., 297 (2016) 183-192.
- [5] M.T. Khorshid, J.B. Ferguson, B.F. Schultz, C.S. Kim, K. Cho, P.K. Rohatgi, Mater. Design., 92 (2016) 79-87.
- [6] Md. Ahasan, M. J. Davidson, Mater. Manuf. Process, 30 (2015) 1190-1195.
- [7] Y.C. Wang, S. Liang, J. Ren, X. Du, F. Liu, Mater. Charact., 121 (2016) 76-81.
- [8] M.Z. Sylwester, Mater. Design., 53 (2014) 758-765.
- [9] F. Wang, Y. Li, X. Wang, Y. Koizumi, Y. Kenta, A. Chiba, J. Alloys Compd., 657 (2016) 122-132.
- [10] M. Krasnowski, S. Gierlotka, T. Kulik, Adv. Powder Technol., 26 (2015) 1269-1272.
- [11] M.R. Akbarpour, JMEPEG, 25 (2016) 1749-1756.
- [12] D. Markó, K.G. Prashanth, S. Scudino, Z. Wang, N. Ellendt, V. Uhlenwinkel, J. Eckert, J. Alloys Compd., 615 (2014) S382-S385.
- [13] Ö. Balci, K.G. Prashanth, S. Scudino, D. Ağaoğulları, İ. Duman, M.L. Öveçoğlu, V. Uhlenwinkel, J. Eckert, Metals, 5 (2015) 669-685.
- [14] Z. Wang, K. Georgarakis, K.S. Nakayama, Y. Li, A.A. Tsarkov, G. Xie, D. Dudina, D.V. Louzguine-Luzgin, A.R. Yavari, Sci. Rep., 6 (2016) 24384.
- [15] T. Wang, Y. Wu, J. Si, X. Hui, Metall. Trans. A, 46 (2015) 2381-2389.
- [16] M. Zhou, K. Hagos, H. Huang, M. Yang, L. Ma, J. Non-Crystall. Solids, 452 (2016) 50-56.
- [17] P. Bhuyan, S.N. Alam, D. Panda, L. Kumar, H. Singh, Materials Today: Proceedings, 4 (2017) 213-223.
- [18] H. Singh, L. Kumar, S.N. Alam, IOP Conf. Series: Mater. Sci. Eng., 75 (2015) 012007.
- [19] K.A. Darling, E.L. Huskins, B.E. Schuster, Q. Wei, L.J. Kecskes, Mater. Sci. Eng. A, 638 (2015) 322-328.
- [20] I. Daoud, Dj. Miroud, R. Yamanoglu, J. Min. Metall. Sect. B-Metall. 54 (2) B (2018) 169 - 177
- [21] J.W. Kaczmar, K. Granat, A. Kurzawa, E. Grodzka, Arch. Foundry. Eng., 14 (2014) 85-90.
- [22] M. Orolínová, J. Ďurišin, K. Ďurišinová, Z. Danková, M. Besterci, Kovove. Mater., 53 (2015) 409-414.
- [23] X.H. Zhang, X.X. Li, H. Chen, T.B. Li, W. Su, S.D. Guo, Mater. Design, 92 (2016) 58-63.
- [24] V. Rajkovic, D. Bozic, M.T. Jovanovic, Mater. Design, 31 (2010) 1962-1970.
- [25] K. Chu, F. Wang, X. Wang, Y. Li, Z. Geng, D. Huang, H. Zhang, Mater. Design, 144 (2018) 290-303
- [26] K. Chu, F. Wang, Y. Li, X. Wang, D. Huang, Z. Geng, Composites Part A 109 (2018) 267-279
- [27] K. Chu, F. Wang, Y. Li, X. Wang, D. Huang, H. Zhang, Carbon 133 (2018) 127-139
- [28] T. Varol, A. Canakci, J. Alloys. Compd., 649 (2015) 1066-1074.
- [29] F.F. Han, A. Inoue, Y. Han, F. L. Kong, S. L. Zhu, E. Shalaan, F. Al-Marzouki, J. Mater. Sci., 52 (2017) 1246-1254.
- [30] Z. Fu, B.E. MacDonald, D. Zhang, B. Wu, W. Chen, J. Ivanisenko, H. Hahn, E.J. Lavernia, Scripta Materialia, 143 (2018) 108-112.
- [31] R.O. Scattergood, C.C. Koch, K.L. Murty, D. Brenner Mat. Sci. Eng. A 493 (2008) 3-11.
- [32] V. Turlo, T.J. Rupert, Acta Materialia 151 (2018) 100-111.
- [33] M. Sveda, A. Sycheva, T. Miko, F. Kristaly, A. Racz, T. Ferenczi, D. Janovszky, J. Non-Crystall. Solids, 473 (2017) 41-46.



- [34] Z. Jiang, H. Kato, T. Ohsuna, J. Saida, A. Inoue, K. Saksl, H. Franz, K. Stahl, Appl. Phys. Lett., 83 (2003) 3299-3301.
- [35] G.E. Abrosimova, A.S. Aronin, J. Surf., Inv. 9 (2015) 887-893.
- [36] K. Durisinova, J. Durisin, M. Durisin, J. Mater. Eng. Perform., 26 (2017) 1057-1061.
- [37] M. Korac, Z. Kamberović, Z. Andić, M. Filipovic, Sintered Materials Based on Copper and Alumina Powders Synthesized by a Novel Method, Nanocomposites and Polymers with Analytical Methods, Dr. John Cuppoletti (Ed.), InTech, Shanghai, 2011, pp. 181-198.
- [38] Copper as electrical conductive material with above-standard performance properties, European Copper Institute, <http://conductivity-app.org>
- [39] S. Nachum, N.A. Flecka, M.F. Ashby, A. Colella, P. Matteazzi, Mater. Sci. Eng. A, 527 (2010) 5065-5071.
- [40] Y.A. Sorkhe, H. Aghajani, A.T. Tabrizi, Powder Metall., 59 (2016) 107-111.
- [41] K.K. Chawla, N. Chawla, Metal-Matrix Composites, in: Kirk-Othmer Encyclopedia of Chemical Technology, John Wiley & Sons, 2000
- [42] Z.F. Zhang, G. He, J. Eckert, L. Schultz, Phys. Rev. Lett., 91 (2003) 045505-1-425.

RAZVOJ NOVIH KOMPOZITNIH MATERIJALA ULTRAFINOG ZRNA SA Cu METALNOM MATRICOM OJAČANIH Ti-Cu-Co-M (M: Ni, Zr) AMORFNIM NANO-KRISTALNIM PRAHOM

D. Janovszky^{a*}, F. Kristaly^b, T. Miko^c, M. Sveda^a, A. Sycheva^a

^a MTA-ME Naučna grupa za istraživanje materijala, Miškolc, Mađarska

^b Institut za mineralogiju i geologiju, Univerzitet u Miškolcu, Miškolc, Mađarska

^c Institut za fizičku metalurgiju, oblikovanje metala i nanotehnologiju, Univerzitet u Miškolcu, Miškolc, Mađarska

Apstrakt

Metalurgijom praha su proizvedeni novi kompozitni materijali ultrafinog zrna sa Cu metalnom matricom, ojačani sa 2-50 wt. % $Ti_{48}Cu_{39.5}Ni_{10}Co_{2.5}$ i $Ti_{48}Cu_{39.5}Zr_{10}Co_{2.5}$ amorfnim nano-kristalnim česticama legura. Karakterizacija kompozita izvršena je uz pomoć optičkog i skenirajućeg elektronskog mikroskopa (SEM), rentgenske difrakcije (XRD), mikro i makro tvrdoće, kao i uz pomoć merenja gustine. Posle toplog valjanja, veličina Cu kristalita je bila manja od 200 nm, i nanokristalna faza praha za ojačavanje je bila 5-35 nm. Gustine od 97-76 % dobijene su u vezi sa proračunatim vrednostima konsolidovanih kompozita, u zavisnosti od udela mase. Uz to, ispitivane su mehaničke osobine i električna otpornost kompozita. Rezultati su pokazali da se 0.2% početna kompresivna čvrstoća na istezanje kompozita povećava dva i pet puta u odnosu na čistu Cu matricu, za kompozite ojačane sa 2 i 50 wt. % ojačavajućih čestica. Električna otpornost stalno raste, sa većim vrednostima posle dodavanja 30 wt. %. Promene u mehaničkim i električnim osobinama su proizvod povećanja amorfnano-kristalnih aditiva.

Ključne reči: Metalurgija praha; Nanostrukturirani materijali; Cu kompoziti; Mehaničke osobine; Mikrostruktura; Amorfn

